1. Introduction

Earlier reports[1–2)] presented the results of preliminary investigations into the production of longitudinal polarization on beam line 4B in the proton experimental hall at TRIUMF. Each of the reports involved the placement of a solenoid between the 35° (at present) vault dipole 4VB1 and the 25° vault dipole 4BVB2. In order to accommodate the solenoid, it is necessary that the section of vault beam line between the combination magnet exit and dipole 4VB1 be shifted some 5° clockwise from its present location. This could be accomplished either by changing the bend angle of the combination magnet by that amount or by the insertion of another dipole downstream of the existing combination magnet. In either case, the use of a single solenoid between the dipoles would yield only partial longitudinal polarization, the degree of which would vary with energy.

Subsequent to the issue of these reports it was suggested[3)] that the addition of another solenoid upstream of dipole 4VB1 might allow the attainment of complete longitudinal polarization. That this, in fact, is so was shown in ref[4)]. Appendix A reproduces the essential arguments of that reference and gives the appropriate formulae from which the required solenoidal fields may be calculated. In addition, formulae relating to the provision of purely (horizontal) transverse polarization are also developed. The latter are required for the section on transverse polarization that follows later.

This report presents a first study of the implementation of the two-solenoid two-dipole system for the production of longitudinal polarization on beam line 4B. Because some experiments would require transverse polarization, a first study of its feasibility is included. Because one would still wish to run the beam line under present-day achromatic and dispersed conditions, tunes for these cases are also given. In this report discussions of the following operating modes will be found:

- vault reconfiguration.
- achromatic operation of beam line 4B.
- dispersed operation of beam line 4B.
- longitudinal polarization on beam line 4B.
- transverse polarization on beam line 4B.

For the latter two cases it is important to stress at the outset that the intent of this report is to show that the production of longitudinal polarization is feasible. Data presented here for them should be regarded as 'preliminary' in the sense that better operational solutions will probably exist. Further, these cases have been considered *only* in the context of beam line operation with *vertical* dispersion at the 4BT2 target location.

Ramifications of the vault reconfiguration on the operation of beam line 4A will be given in a subsequent report.

2. Vault reconfiguration

As was noted above, in order that sufficient room between the vault dipoles for the insertion of a solenoid be obtained, it is necessary to either change the bend angle of the combination magnet or to add another

dipole in the vault. The procedure adopted here is the former.

It has been shown [5] that extraction of beam into the vault section of beam line 4 is possible if the bend angle of the combination magnet is reduced by 5°. In figure 1 the (revised) vault configuration considered for data presented here is shown. Vault quadrupoles 4VQ1 and 4VQ2 have been rotated 5° clockwise from their present locations relative to the exit of the combination magnet. Thus their positions relative to the combination magnet do not change (other than the 5° rotation, of course). Quadrupole 4VQ3 has been repositioned such that its center lies 1.4064 m downstream of that of quadrupole 4VQ2. The center of the first solenoid, 4VSOL1, lies 1.4027 m downstream of that of 4VQ3. The second vault solenoid, 4VSOL2, is centered between the two dipoles. It is to be noted that the bend angle of 4VB1 is now increased from 35° to 40°.

Because the bend angle of the combination magnet has been lowered, extraction parameters into the vault section will also change. Table 1 gives the input phase-space parameters, the new extraction parameters, and, for comparison, those currently in use. It is seen that the reduction of the bend angle of the combination magnet significantly affects only the angular dispersion term R_{16}.

3. Achromatic operation on beam line 4B

For achromatic operation of the beam line the solenoids are turned off and are treated as drift lengths. Table 2 lists the beam transport settings for energies of 200, 300, 400, and 500 MeV. Beam parameters and overall transfer matrix elements at 4BT1 are listed in table 3. Beam sizes at 4BT2 will be either identical or interchanged between x and y depending on the orientation of the twister. Figures 2–5 show the computed beam envelopes for the various energies.

4. Dispersed operation on beam line 4B

In dispersed operation of the beam line the solenoids are turned off and are treated as drift lengths. A horizontally dispersed beam is obtained at the target location 4BT1 and, depending on the orientation of the twister, either a horizontally or vertically dispersed beam is produced at 4BT2. Beam transport parameters for a dispersed beam-line tune are given in table 4 for beam energies of 200, 300, 400, and 500 MeV. Table 5 lists the beam sizes and the overall transfer matrices at 4BT1 and 4BT2 for the case of vertical dispersion at the MRS target. Computed beam profiles along the line are shown in figures 6–9.

5. Longitudinal polarization on beam line 4B

In this case the vault solenoids are turned on at the values calculated from the formulae given in ref [4]. When this is done not only are the spins of the particles precessed into a direction along the beam axis, but the phase-space of the beam is also rotated with respect to the normal laboratory coordinate system. After passing through the first solenoid the (x,θ) and (y,ϕ) phase spaces are coupled. Were the beam extracted from the cyclotron dispersionless, an explicit momentum dependence would exist in only the horizontal position and divergence at the exit of the first dipole. The second solenoid would would then couple the horizontal-plane momentum dependence to the vertical coordinates. Consequently, on exiting from the second dipole the spatial coordinates of the beam particles would be completely mixed. Because of the dispersion present in the beam at extraction, however, the first solenoid introduces dispersion into both the horizontal and vertical planes. Thus all spatial coordinates of beam particles have momentum dependence on exiting the second dipole regardless of the characteristics of the extracted beam.

The coupling of the (initially) independent $(x,\theta,\delta p)$ and (y,ϕ) phase spaces can be overcome by deliberately rotating phase space to counteract that induced by the solenoid-dipole solenoid-dipole configuration. The twister on beam line 4B was designed such that it rotates about the beam axis in order that the spatial coupling induced in (horizontal) transverse polarization be counteracted. Another possibility is to rotate other quadrupoles in the beam line. In particular, if one rotated quadrupoles 4VQ1 and 4VQ2—that lie

upstream on the first solenoid—one might be able to better offset the phase-space rotation induced in the production of longitudinal polarization.

Toward this end, designs were obtained for longitudinal polarization utilizing twister rotation combined with either with or without vault quadrupole rotation. These will be presented separately below. In each case, however, it was decided to force the following conditions at 4BT2:

- a horizontal waist.
- $R_{11} = R_{12} = R_{16} = 0$.
- $R_{21} = R_{12} = 0$.
- $R_{32} = R_{33} = R_{34} = 0$.
- $R_{36} = -10$ cm/%.
- $R_{43} = R_{44} = 0$.

5.1 Longitudinal polarization with vault quadrupole rotation

Here, vault quadrupoles 4VQ1 and 4VQ2 are rotated together. Beam transport parameters, including the required rotation angles of the vault quadrupoles and of the twister, are given in table 6. Remember that this case corresponds to *vertically* dispersed beam at 4BT2.

Table 7 lists the beam parameters and the overall transfer matrices at 4BT1; those at the 4BT2 location are given in table 8. Beam profiles along the line are shown in figures 10–13.

5.2 Longitudinal polarization without vault quadrupole rotation

In this case, vault quadrupoles 4VQ1 and 4VQ2 are not rotated from their standard orientation. The twister, however, is allowed to rotate about the beam axis in order to decouple the horizontal and vertical phase spaces.

Beam transport parameters, including the required rotation angle of the twister, are given in table 9. Table 10 lists the the beam parameters and the overall transfer matrices at 4BT1; those at the 4BT2 location are given in table 11. Beam profiles along the line are shown in figures 14–17.

5.3 Discussion of the longitudinal polarization schemes

the studies discussed above have shown that the production of longitudinal polarization along beam line 4B is feasible. There are, however, several points to note.

The only position outside of the cyclotron vault at which vertical and horizontal phase spaces are decoupled is at the 4BT2 (MRS) target location. This can only indicate that the tuning of the beam line under conditions of longitudinal polarization will be extremely difficult. It will be necessary to know the characteristics of the beam line extremely well in order that one is confident that the Hall-plate readings can be relied upon to produce the desired optics.

Further, reference to tables 6 and 9 indicates that if the vault-quadrupole rotation scheme were used, quadrupoles 4BQ9 and 4BQ10 require pole-tip fields that are just reachable with the present power supplies. On the other hand, rotation of the twister quadrupoles *only* requires that the two middle quadrupoles of the twister have fields higher than presently attainable. In this case, it would probably be necessary to replace that pair of quadrupoles with a pair of the 'long' 4-inch design.

These tables also indicate a peculiarity of the solutions presented here. In the vault-rotation scheme

quadrupole 4VQ3 reverses polarity between 300 MeV and 400 MeV. Moreover, its pole-tip field appears anomalously high at the lower energy. If vault quadrupoles are not rotated, table 9 shows that this still occurs and that under these circumstances it is also necessary to reverse quadrupole 4VQ1 between 400 MeV and 500 MeV. Table 11 also indicates that it is necessary to decouple quadrupoles 4BQ9 and 4BQ10 at 200 MeV.

Whether these are anomalies or requirements for the production of longitudinal polarization will become clear with more detailed study of the optics of the beam line.

6. Horizontal transverse polarization on beam line 4B

At the present time horizontal transverse polarization is provided on beam line 4B with the installation of a solenoid outside the vault wall upstream of target position 4BT1. Such a solenoid will couple horizontal, vertical, and momentum phase spaces. This coupling is removed by the rotation of the twister about the beam axis. Were, however, the provision of longitudinal polarization made on the beam line, the vault solenoids could be used to generate transverse polarization, thus avoiding the cost of another solenoid and/or the time required to remove a solenoid from the vault and to insert it into the beam line in the experimental area.

The method of ref[4)] is used in Appendix A to develop the appropriate formulae for the provision of horizontal transverse polarization for the beam line. These formulae are used to give the beam-line parameters listed in table 12. At the time of writing, only solutions requiring the rotation of vault quadrupoles have been obtained for all extracted energies. Solutions not requiring vault-quadrupole rotation will be reported at a later date.

Beam parameters and overall transfer matrices at target positions 4BT1 and 4BT2 are given in tables 13 and 14 respectively. Once again it is noted that the only point at which vertical and horizontal phase spaces are completely decoupled is at the 4BT2 target position. Figures 18–21 indicate the expected beam profiles along the beam line at the various energies.

7. Discussion

Let it be emphasized again that the intent of this report has been to discuss the feasibility of the production of longitudinal and transverse polarizations using a two-solenoid two-dipole system on beam line 4B. It was not the intent to produce a final, definitive set of operating parameters.

It was necessary to show that one would still be able to run the beam line as it is now run—that is, in 'standard' achromatic and dispersed modes of operation. Data presented in §3 and §4 indicate that such is possible.

The production of longitudinal polarization was discussed in §5. It was shown that it was possible to produce such polarization without the requirement of major changes to any beam-line components outside of the cyclotron vault. It was indicated, however, that the beam line would be difficult to tune and that it might be necessary to change the two middle quadrupoles of the twister. Similarly, as was indicated in §6, there would not appear to be any problem in the production of transverse polarization on the beam line, although the tuning problem would, however, still exist (as it would were a single solenoid be located outside of the vault wall).

It can now be stated that the two-solenoid two-dipole system may be used on beam line 4B for the production of both longitudinal and transverse polarizations. A more detailed study of the optics of the beam line is, however, required.

References

1. G. M. Stinson, TRIUMF report TRI-DNA-83-7.
2. G. M. Stinson, TRIUMF report TRI-DNA-83-8.
3. G. Dutto, 'Inspired remark', TRIUMF, March, 1984.
4. M. K. Craddock, TRIUMF report TRI-DN-84-8.
5. C. J. Kost, *Private communication*, TRIUMF, Spring 1984.

Appendix A

In this section the results obtained in ref[4)] for the production of longitudinal polarization by a two-solenoid two-dipole system are reproduced. The technique is then used to develop a prescription for the production of horizontal transverse polarization with the same configuration of elements.

A1. Longitudinal polarization with a two-solenoid two-dipole system.

The following figure, taken from ref[4)], indicates the process by which a vertically polarized beam is transformed into a longitudinally polarized beam by a solenoid-dipole solenoid-dipole system. In the figure the beam is directed along the positive y-axis. Illustrated is the following sequence:

- precession of the spin through an angle ϕ_1 clockwise about the y-axis in the first solenoid.
- precession of the spin through an angle $\Theta_1 = \gamma G\theta_1$ clockwise about the z-axis in the first dipole.
- precession of the spin through an angle ϕ_2 clockwise about the y-axis in the second solenoid.
- precession of the spin through an angle $\Theta_2 = \gamma G\theta_2$ about the z-axis in the second dipole.

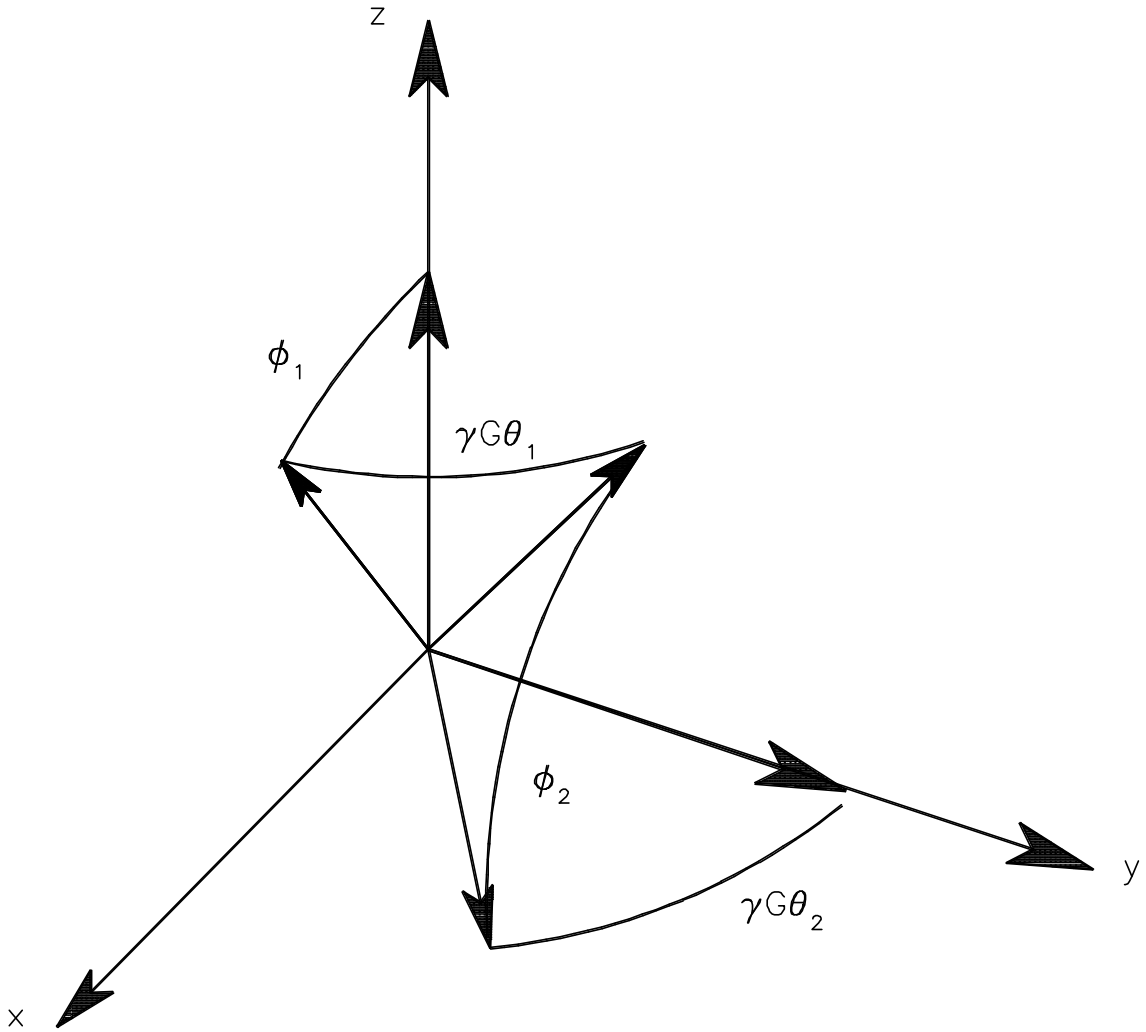

Fig. A1. The process of producing longitudinal polarization with a solenoid-dipole solenoid-dipole system.

In the above: $G = (g/2 - 1) = 1.79285$ for protons.
θ_1 = bend angle of the first dipole
θ_2 = bend angle of the second dipole

After passing through the first solenoid and then the first dipole, the net precession of spin is obtained from

$$\begin{bmatrix} 0 \\ 0 \\ 1 \end{bmatrix} \quad \text{Solenoid 1} \longrightarrow \quad \begin{bmatrix} \sin(\phi_1) \\ 0 \\ \cos(\phi_1) \end{bmatrix} \quad \text{Dipole 1} \longrightarrow \quad \begin{bmatrix} \sin(\phi_1)\cos(\Theta_1) \\ \sin(\phi_1)\sin(\Theta_1) \\ \cos(\phi_1) \end{bmatrix} . \tag{1}$$

Similarly, working backwards through the second dipole and then the second solenoid, one obtains

$$\begin{bmatrix} \sin(\Theta_2)\cos(\phi_2) \\ \cos(\Theta_2) \\ \sin(\Theta_2)\sin(\phi_2) \end{bmatrix} \quad \text{Solenoid 2} \longleftarrow \quad \begin{bmatrix} \sin(\Theta_2) \\ \cos(\Theta_2) \\ 0 \end{bmatrix} \quad \text{Dipole 2} \longleftarrow \quad \begin{bmatrix} 0 \\ 1 \\ 0 \end{bmatrix} . \tag{2}$$

Demanding that the spin vectors be equal between the first dipole and the second solenoid produces the relation

$$\begin{bmatrix} \sin(\phi_1)\cos(\Theta_1) \\ \sin(\phi_1)\sin(\Theta_1) \\ \cos(\phi_1) \end{bmatrix} = \begin{bmatrix} \sin(\Theta_2)\cos(\phi_2) \\ \cos(\Theta_2) \\ \sin(\Theta_2)\sin(\phi_2) \end{bmatrix} \tag{3}$$

from which it follows that

$$\sin(\phi_1) = \frac{\cos(\Theta_2)}{\sin(\Theta_1)} \tag{4}$$

and

$$\cos(\phi_2) = \frac{1}{\tan(\Theta_1) \cdot \tan(\Theta_2)} . \tag{5}$$

The spin precession angle ϕ is related to the solenoid properties through

$$\phi = \mu\,\Phi = \mu\,\frac{B_0 L}{(B\rho)_0} \tag{6}$$

in which:

μ	=	the magnetic moment of the particle,
B_0	=	the axial field of the solenoid,
L	=	the effective length of the solenoid,
$(B\rho)_0$	=	magnetic rigidity of the particle.

It is noted that if the spin is precessed through an angle $\phi = \mu\,\Phi$, phase space is rotated through an angle given by

$$\alpha = \frac{\Phi}{2} = \frac{B_0 L}{2(B\rho)_0} . \tag{7}$$

For reference, table A1(a) lists the solenoidal fields required for the production of longitudinal polarization on beam line 4B as a function of energy.

A2. Transverse polarization with a two-solenoid two-dipole system

In this instance one desires that the spin be rotated into the horizontal plane. The sequence given by equation 1 is still valid, but now that given by equation 2 is replaced with

$$\begin{bmatrix} \cos(\Theta_2)\cos(\phi_2) \\ -\sin(\Theta_2) \\ \cos(\Theta_2)\sin(\phi_2) \end{bmatrix} \quad \text{Solenoid 2} \quad \begin{bmatrix} \cos(\Theta_2) \\ -\sin(\Theta_2) \\ 0 \end{bmatrix} \quad \text{Dipole 2} \quad \begin{bmatrix} 1 \\ 0 \\ 0 \end{bmatrix} . \tag{8}$$

Again, the requirement that the spin vectors be equal between the first dipole and the second solenoid produces the relation

$$\begin{bmatrix} \sin(\phi_1)\cos(\Theta_1) \\ \sin(\phi_1)\sin(\Theta_1) \\ \cos(\phi_1) \end{bmatrix} = \begin{bmatrix} \cos(\Theta_2)\cos(\phi_2) \\ -\sin(\Theta_2) \\ \cos(\Theta_2)\sin(\phi_2) \end{bmatrix} \tag{9}$$

from which it follows that

$$\sin(\phi_1) = -\frac{\sin(\Theta_2)}{\sin(\Theta_1)} \tag{10}$$

and

$$\cos(\phi_2) = -\frac{\tan(\Theta_2)}{\tan(\Theta_1)} . \tag{11}$$

The relations given in equations 6 and 7 may then be used to determine the required solenoid fields and the accompanying phase-space rotation.

Listed in table A1(b) are the solenoid fields required for the production of horizontal transverse polarization on beam line4B.

Table 1

Input phase space and computed extraction parameters for extraction port 4
– Present and proposed vault configurations –

	500 MeV		400 MeV	
$\pm x$ (cm)	0.127		0.127	
$\pm\theta$ (mr)	1.600		1.600	
$\pm y$ (cm)	0.669		0.481	
$\pm\phi$ (mr)	0.556		0.522	
	Present	Proposed	Present	Proposed
R_{11} (cm/cm)	−0.10000	−0.12790	0.15190	0.23670
R_{12} (cm/mr)	0.32723	0.31660	0.39224	0.40448
R_{16} (cm/%)	1.21600	1.26730	1.89270	1.97770
R_{21} (mr/cm)	−3.11200	−3.28600	−2.39600	−2.31900
R_{22} (mr/mr)	0.14440	0.13230	0.19160	0.24770
R_{26} (mr/%)	1.15700	2.15100	0.95900	2.14400
R_{33} (cm/cm)	1.09300	1.10600	0.89000	0.84000
R_{34} (cm/mr)	0.63693	0.63495	0.61130	0.60030
R_{43} (mr/cm)	0.37000	0.44000	−0.46000	−0.39000
R_{44} (mr/mr)	1.13200	1.15500	0.81000	0.91400

	300 MeV		200 MeV	
$\pm x$ (cm)	0.127		0.127	
$\pm\theta$ (mr)	2.100		2.560	
$\pm y$ (cm)	0.402		0.512	
$\pm\phi$ (mr)	0.401		0.354	
	Present	Proposed	Present	Proposed
R_{11} (cm/cm)	4.24080	4.33020	4.16680	4.02550
R_{12} (cm/mr)	1.16798	1.17567	1.44871	1.39844
R_{16} (cm/%)	3.79620	3.79820	4.76380	4.60020
R_{21} (mr/cm)	4.36800	4.73300	4.13000	3.99000
R_{22} (mr/mr)	1.42190	1.50940	1.65610	1.62980
R_{26} (mr/%)	2.89500	4.03500	2.67700	3.52000
R_{33} (cm/cm)	−1.45600	−1.50000	−0.74300	−0.79000
R_{34} (cm/mr)	0.16350	0.16800	0.75200	0.23140
R_{43} (mr/cm)	−2.95000	−3.73000	−1.02000	−1.77000
R_{44} (mr/mr)	−0.35500	−0.24800	−0.90500	−0.71300

Table 2

Beam line 4B transport parameters for achromatic operation

Element	Fields in kG at energy (MeV)			
	500	400	300	200
4VQ1	8.78360	5.90101	3.80162	2.79949
4VQ2	−4.60798	−3.96915	−3.28136	−2.85856
4VQ3	3.94712	3.60504	3.41179	2.83126
4VB1	16.24183	14.21829	12.03994	9.60203
4BVB2	10.13620	8.87335	7.51384	5.99240
4BQ4	3.50534	2.96853	2.69671	1.91741
4BQ5	−4.00520	−3.25608	−2.90766	−1.83733
4VQ7	5.12704	4.48828	3.80064	3.03105
4VQ8	−7.00467	−6.13198	−5.19251	−4.14110
4VQ9	8.00000	7.00329	5.93033	4.72953
4VQ10	8.00000	7.00329	5.93033	4.72953
4VQ11	−7.00467	−6.13198	−5.19251	−4.14110
4VQ12	5.12704	4.48828	3.80064	3.03105
4VQ13	−4.58818	−4.01659	−3.40124	−2.71261
4VQ14	4.92218	4.30898	3.64883	2.91008

Table 3

Beam sizes and transfer matrix elements at 4BT1[†] in achromatic operation

Parameter	Energy (MeV)			
	500	400	300	200
$\pm x$ (cm)	0.092	0.106	0.085	0.107
$\pm\theta$ (mr)	2.294	1.960	3.116	3.078
$\pm y$ (cm)	0.143	0.269	0.111	0.274
$\pm\phi$ (mr)	1.456	0.710	1.727	1.261
R_{11} (cm/cm)	−0.7225	−0.8173	−0.6435	−0.8237
R_{12} (cm/mr)	0.0036	0.0119	0.0107	0.0083
R_{16} (cm/%)	0.0001	0.0000	0.0000	0.0000
R_{21} (mr/cm)	−1.1431	−2.8257	−6.6011	−4.9714
R_{22} (mr/mr)	−1.4107	−1.1783	−1.4005	−1.1410
R_{26} (mr/%)	0.0001	0.0000	0.0001	−0.0001
R_{33} (cm/cm)	−0.2439	0.0272	0.2440	0.4373
R_{34} (cm/mr)	−0.4165	−0.4177	0.2292	0.3684
R_{43} (mr/cm)	3.5441	2.3069	−3.7051	−1.7823
R_{44} (mr/mr)	1.9592	1.4092	0.6129	0.7870

[†] Beam sizes calculated for phase spaces listed in Table 1.

Table 4

Beam line 4B transport parameters for dispersed operation

Element	Fields in kG at energy (MeV)			
	500	400	300	200
4VQ1	5.74267	4.21391	3.06421	2.60040
4VQ2	−4.74434	−4.30675	−2.84895	−3.28075
4VQ3	2.43344	2.56693	3.11179	2.63216
4VB1	16.24183	14.21829	12.03994	9.60203
4BVB2	10.13620	8.87335	7.51384	5.99240
4BQ4	2.40534	1.95890	2.30671	0.75707
4BQ5	−2.52453	−1.95614	−3.03733	−0.63730
4VQ7	5.12704	4.48828	3.80064	3.03105
4VQ8	−7.00467	−6.13198	−5.19251	−4.14110
4VQ9	8.00000	7.00329	5.93033	4.72953
4VQ10	8.00000	7.00329	5.93033	4.72953
4VQ11	−7.00467	−6.13198	−5.19251	−4.14110
4VQ12	5.12704	4.48828	3.80064	3.03105
4VQ13	−4.58818	−4.01659	−3.40124	−2.71261
4VQ14	4.92218	4.30898	3.64883	2.91008

Table 5

Beam sizes and transfer matrix elements at 4BT1[†] in dispersed operation

Parameter	Energy (MeV)			
	500	400	300	200
$\pm x$ (cm)	1.005	1.009	1.005	1.011
$\pm\theta$ (mr)	2.073	1.549	2.768	2.215
$\pm y$ (cm)	0.137	0.244	0.128	0.278
$\pm\phi$ (mr)	1.521	0.784	1.489	1.245
R_{11} (cm/cm)	0.8021	1.0587	0.7759	1.1978
R_{12} (cm/mr)	0.0	0.0	0.0	0.0
R_{16} (cm/%)	−10.0000	−10.0000	−10.0000	−10.0000
R_{21} (mr/cm)	0.6441	1.3875	4.8759	2.8059
R_{22} (mr/mr)	1.2760	0.9414	1.2522	0.8190
R_{26} (mr/%)	0.0	0.0	−2.6188	−3.1861
R_{33} (cm/cm)	−0.2211	0.1272	0.2874	0.4357
R_{34} (cm/mr)	−0.3916	−0.3123	0.2629	0.3762
R_{43} (mr/cm)	3.7955	2.5158	−3.1399	−1.7954
R_{44} (mr/mr)	2.2072	1.7008	0.6028	0.7465

[†] Beam sizes calculated for phase spaces listed in Table 1.

Table 6

Beam line 4B transport parameters for longitudinal polarization *with* vault quadrupole rotation†

Element	Fields in kG at energy (MeV)			
	500	400	300	200
Quad. rot'n (°)	−3.84239	−3.41270	−1.77740	−2.47665
4VQ1	2.59047	2.09923	2.80547	2.26149
4VQ2	−1.92468	−1.06800	−3.73971	−2.66829
Quad. rot'n (°)	3.84239	3.41270	1.77740	2.47665
4VQ3	−2.33037	−2.14684	6.80198	3.29741
4VSOL1	8.74435	9.00432	8.83153	8.11717
4VB1	16.24183	14.21829	12.03994	9.60203
4VSOL2	37.75604	32.37555	26.46350	19.98295
4BVB2	10.13620	8.87335	7.51384	5.99240
4BQ4	1.80083	1.90671	1.73121	1.34206
4BQ5	−1.54435	−1.89580	−2.06353	−1.60919
Quad. rot'n (°)	38.60158	39.98176	43.59071	47.40330
4VQ7	5.12704	4.48828	3.80064	3.03105
4VQ8	−7.00467	−6.13198	−5.19251	−4.14110
4VQ9	8.00000	7.00329	5.93033	4.72953
4VQ10	8.00000	7.00329	5.93033	4.72953
4VQ11	−7.00467	−6.13198	−5.19251	−4.14110
4VQ12	5.12704	4.48828	3.80064	3.03105
Quad. rot'n (°)	−38.60158	−39.98176	−43.59071	−47.40330
4VQ13	−4.58818	−4.01659	−3.40124	−2.71261
4VQ14	4.92218	4.30898	3.64883	2.91008

† Solenoid fields calculated for solenoids of 0.59055 m effective lengths.

Table 7

Beam sizes and transfer matrix elements at 4BT1† for longitudinal polarization *with* vault quadrupole rotation†

Parameter	Energy (MeV)			
	500	400	300	200
$\pm x$ (cm)	0.944	0.991	1.507	1.513
$\pm\theta$ (mr)	1.177	0.998	1.411	1.782
$\pm y$ (cm)	0.394	0.333	0.863	1.516
$\pm\phi$ (mr)	0.840	0.944	1.387	1.321
R_{11} (cm/cm)	1.6744	1.2622	1.0336	0.3889
R_{12} (cm/mr)	−0.0411	−0.0920	−0.1657	−0.2344
R_{13} (cm/cm)	−0.4261	−0.5266	2.4615	1.7146
R_{14} (cm/mr)	−0.3815	−0.6320	0.0282	0.0316
R_{16} (cm/%)	−9.0566	−9.3154	−10.8112	−10.7235
R_{21} (mr/cm)	6.3730	4.8695	1.4482	1.9888
R_{22} (mr/mr)	0.4349	0.4263	0.4133	0.5646
R_{23} (mr/cm)	0.3296	−0.0982	2.1856	1.4874
R_{24} (mr/mr)	0.2189	−0.1378	0.1521	0.2031
R_{26} (mr/%)	−4.6447	−3.5422	−6.9579	−6.1597
R_{31} (cm/cm)	−1.2567	−1.1006	−0.6045	−1.3691
R_{32} (cm/mr)	−0.0612	−0.1058	−0.3322	−0.5426
R_{33} (cm/cm)	−0.4796	0.1163	1.3153	0.9026
R_{34} (cm/mr)	−0.7821	−0.3088	0.2003	0.3331
R_{36} (cm/%)	2.2649	0.7038	−1.0405	−1.7797
R_{41} (mr/cm)	−2.0292	−1.7959	0.3044	−0.2750
R_{42} (mr/mr)	−0.1253	−0.1821	−0.3361	−0.3246
R_{43} (mr/cm)	1.8258	2.4070	−2.8222	−1.8868
R_{44} (mr/mr)	0.9653	2.1345	0.0917	0.0787
R_{46} (mr/%)	0.9874	−1.0969	−2.0440	−1.6853

† Beam sizes calculated for phase spaces listed in Table 1.

Table 8

Beam sizes and transfer matrix elements at 4BT2† for longitudinal polarization *with* vault quadrupole rotation†

Parameter	Energy (MeV)			
	500	400	300	200
$\pm x$ (cm)	0.280	0.229	0.115	0.259
$\pm\theta$ (mr)	0.752	0.849	1.736	1.398
$\pm y$ (cm)	1.044	1.038	1.021	1.013
$\pm\phi$ (mr)	0.946	1.454	1.598	2.193
R_{13} (cm/cm)	−0.3172	0.6033	0.1854	0.1229
R_{14} (cm/mr)	−0.7137	0.1443	0.2397	0.3771
R_{16} (cm/%)	0.0	0.0	0.0	0.0
R_{23} (mr/cm)	2.0432	1.5866	−4.3646	−2.7730
R_{24} (mr/mr)	1.4500	2.0401	−0.2572	−0.3653
R_{26} (mr/%)	−1.1210	−1.4432	4.7315	4.1410
R_{31} (cm/cm)	2.3513	2.1948	1.6325	1.2521
R_{32} (cm/mr)	0.0	0.0	0.0	0.0
R_{36} (cm/%)	−10.0000	−10.0000	−10.0000	−10.0000
R_{41} (mr/cm)	4.7776	1.6314	−0.5652	1.1844
R_{42} (mr/mr)	0.4353	0.4541	0.5951	0.7835
R_{46} (mr/%)	2.3445	12.3234	9.5980	7.1119

† Beam sizes calculated for phase spaces listed in Table 1.

Table 9

Beam line 4B transport parameters for longitudinal polarization *with no* vault quadrupole rotation†

Element	Fields in kG at energy (MeV)			
	500	400	300	200
Quad. rot'n (°)	0.0	0.0	0.0	0.0
4VQ1	−2.04349	0.43809	2.80090	2.32201
4VQ2	4.53076	2.45462	−3.86532	−2.75773
Quad. rot'n (°)	0.0	0.0	0.0	0.0
4VQ3	−2.33037	−2.04538	6.80198	2.50590
4VSOL1	8.74435	9.00432	8.83153	8.11717
4VB1	16.24183	14.21829	12.03994	9.60203
4VSOL2	37.75604	32.37555	26.46350	19.198295
4BVB2	10.13620	8.87335	7.51384	5.99240
4BQ4	2.29589	2.00655	1.61604	1.20785
4BQ5	−2.52504	−2.20306	−1.81181	−1.39190
Quad. rot'n (°)	37.91444	39.12658	39.55474	41.52960
4VQ7	5.41486	4.73548	3.97015	3.15004
4VQ8	−7.51275	−6.57069	−5.54817	−4.41474
4VQ9	11.76019	10.27448	8.86398	7.23862
4VQ10	11.76019	10.27448	8.86398	7.23862
4VQ11	−7.51275	−6.57069	−5.54817	−4.41474
4VQ12	5.41486	4.73548	3.97015	3.15004
Quad. rot'n (°)	−37.91444	−39.12658	−39.55474	−41.52960
4VQ13	−4.58818	−4.01659	−3.40124	−2.71261
4VQ14	4.92218	4.30898	3.64883	2.91008

† Solenoid fields calculated for solenoids of 0.59055 m effective lengths.

Table 10

Beam sizes and transfer matrix elements at 4BT1† for longitudinal polarization *with no* vault quadrupole rotation†

Parameter	Energy (MeV)			
	500	400	300	200
$\pm x$ (cm)	1.286	1.473	1.193	1.506
$\pm\theta$ (mr)	1.450	1.497	1.379	2.278
$\pm y$ (cm)	0.605	0.735	0.639	1.371
$\pm\phi$ (mr)	1.556	1.941	1.255	1.888
R_{11} (cm/cm)	0.8445	0.3567	0.8430	−0.0407
R_{12} (cm/mr)	−0.2981	−0.2794	−0.2000	−0.3125
R_{13} (cm/cm)	−0.8587	−1.7862	1.1027	0.9232
R_{14} (cm/mr)	−1.0295	−2.0008	0.1472	0.1238
R_{16} (cm/%)	−11.4152	−11.4805	−10.3389	−11.7944
R_{21} (mr/cm)	0.5201	1.9963	1.8163	2.8104
R_{22} (mr/mr)	0.8654	0.8243	0.5607	0.8212
R_{23} (mr/cm)	−0.4208	−1.1517	0.8418	0.6507
R_{24} (mr/mr)	−0.6602	−1.3674	0.2388	0.2378
R_{26} (mr/%)	−2.7896	−2.3809	−5.7044	−5.1383
R_{31} (cm/cm)	−0.0566	−0.6323	−0.5758	−1.4033
R_{32} (cm/mr)	−0.3344	−0.3206	−0.2701	−0.4944
R_{33} (cm/cm)	−0.1365	−0.9185	0.7649	0.3925
R_{34} (cm/mr)	−0.5036	−1.1943	0.4217	0.5150
R_{36} (cm/%)	−1.2130	−1.3495	−0.3623	−1.4535
R_{41} (mr/cm)	0.2784	−0.9890	−0.4884	−1.4979
R_{42} (mr/mr)	−0.7765	−0.9890	−0.4646	−0.6248
R_{43} (mr/cm)	2.2821	3.5366	−1.5970	−1.4488
R_{44} (mr/mr)	2.0858	3.6580	0.2429	0.2949
R_{46} (mr/%)	−4.9206	−5.0874	−1.9482	−2.8345

† Beam sizes calculated for phase spaces listed in Table 1.

Table 11

Beam sizes and transfer matrix elements at 4BT2[†] for longitudinal polarization *with no* vault quadrupole rotation[†]

Parameter	Energy (MeV)			
	500	400	300	200
$\pm x$ (cm)	0.286	0.101	0.233	0.405
$\pm\theta$ (mr)	0.749	1.897	0.844	0.884
$\pm y$ (cm)	1.006	1.007	1.014	1.006
$\pm\phi$ (mr)	2.860	2.789	2.136	3.483
R_{13} (cm/cm)	0.5708	0.2482	0.1744	−0.1285
R_{14} (cm/mr)	0.1901	0.0403	0.4540	0.5075
R_{16} (cm/%)	0.0	0.0	0.0	0.0
R_{23} (mr/cm)	1.6021	4.0340	−2.4457	−1.8013
R_{24} (mr/mr)	2.2825	4.6914	−0.6410	−0.6739
R_{26} (mr/%)	1.8066	1.9188	1.9722	2.2404
R_{31} (cm/cm)	0.8964	0.9236	1.3316	0.8321
R_{32} (cm/mr)	0.0	0.0	0.0	0.0
R_{36} (cm/%)	−10.0000	−10.0000	−10.0000	−10.0000
R_{41} (mr/cm)	−1.5257	0.3981	−0.4435	2.2335
R_{42} (mr/mr)	1.1416	1.0790	0.7296	1.1785
R_{46} (mr/%)	21.7019	21.5981	14.5310	15.4028

[†] Beam sizes calculated for phase spaces listed in Table 1.

Table 12

Beam line 4B transport parameters for transverse polarization *with* vault quadrupole rotation†

Element	Fields in kG at energy (MeV)			
	500	400	300	200
Quad. rot'n (°)	−7.48168	−10.56223	−0.77547	4.18353
4VQ1	4.05579	3.79125	2.90234	2.22516
4VQ2	−4.05677	−3.97510	−3.53461	−2.50757
Quad. rot'n (°)	7.48168	10.56223	0.77547	−4.18353
4VQ3	1.72593	1.16102	2.65815	2.32429
4VSOL1	−31.67773	−22.50786	−16.96190	−12.39378
4VB1	16.24183	14.21829	12.03994	9.60203
4VSOL2	8.29970	21.41594	23.44341	21.42796
4BVB2	10.13620	8.87335	7.51384	5.99240
4BQ4	2.42021	1.73282	1.48205	1.18109
4BQ5	−2.49502	−1.59689	−1.51082	−1.49113
Quad. rot'n (°)	44.17994	41.42781	39.25907	30.61625
4VQ7	5.10868	4.44375	4.11882	3.36157
4VQ8	−7.13708	−6.23183	−5.05817	−4.60485
4VQ9	8.65949	7.79022	4.05061	6.89720
4VQ10	8.65949	7.79022	4.05061	6.89720
4VQ11	−7.13708	−6.23183	−5.05817	−4.60485
4VQ12	5.10868	4.44375	4.11882	3.36157
Quad. rot'n (°)	−44.17994	−41.42781	−39.25907	−30.61625
4VQ13	−4.58818	−4.01659	−3.40124	−2.71261
4VQ14	4.92218	4.30898	3.64883	2.91008

† Solenoid fields calculated for solenoids of 0.59055 m effective lengths.

Table 13

Beam sizes and transfer matrix elements at 4BT1† for transverse polarization *with* vault quadrupole rotation†

Parameter	Energy (MeV)			
	500	400	300	200
$\pm x$ (cm)	0.972	0.981	1.028	1.784
$\pm\theta$ (mr)	1.405	2.166	2.770	2.178
$\pm y$ (cm)	0.171	0.381	0.427	0.376
$\pm\phi$ (mr)	1.406	0.673	1.370	3.693
R_{11} (cm/cm)	1.1196	0.6263	0.4710	−0.0621
R_{12} (cm/mr)	−0.0530	−0.0755	−0.0725	−0.3959
R_{13} (cm/cm)	−0.1044	−0.0538	−0.1530	0.8685
R_{14} (cm/mr)	−0.0895	−0.1307	0.1289	0.4401
R_{16} (cm/%)	−9.5733	−9.6776	−10.0711	−13.7886
R_{21} (mr/cm)	1.5631	2.5114	4.9463	2.8765
R_{22} (mr/mr)	0.8522	1.3030	1.2542	0.7455
R_{23} (mr/cm)	0.1021	0.0127	−0.2854	0.9099
R_{24} (mr/mr)	0.2139	0.2009	0.0899	0.3301
R_{26} (mr/%)	−1.2218	1.9108	−1.5876	−7.4278
R_{31} (cm/cm)	0.0100	−0.2013	0.5411	−0.0395
R_{32} (cm/mr)	−0.0175	−0.0754	0.1646	−0.0463
R_{33} (cm/cm)	−0.4213	0.3433	0.5649	0.7032
R_{34} (cm/mr)	−0.5393	−0.3329	0.3085	0.3719
R_{36} (cm/%)	0.0311	0.8092	1.2972	−0.2961
R_{41} (mr/cm)	−0.7433	−0.6691	−1.2522	−3.4905
R_{42} (mr/mr)	−0.0499	−0.2055	−0.3393	−1.2656
R_{43} (mr/cm)	3.5677	1.8516	−2.4561	−2.5475
R_{44} (mr/mr)	2.1665	1.1496	0.3859	0.2398
R_{46} (mr/%)	−3.5824	−0.8375	−1.7547	−5.9861

† Beam sizes calculated for phase spaces listed in Table 1.

Table 14

Beam sizes and transfer matrix elements at 4BT2† for transverse polarization *with* vault quadrupole rotation†

Parameter	Energy (MeV)			
	500	400	300	200
$\pm x$ (cm)	0.154	0.366	0.167	0.299
$\pm\theta$ (mr)	1.450	0.650	1.155	1.208
$\pm y$ (cm)	1.012	1.005	1.005	1.005
$\pm\phi$ (mr)	1.463	2.217	3.182	6.638
R_{13} (cm/cm)	−0.2038	0.4583	0.4211	−0.3311
R_{14} (cm/mr)	−0.4135	−0.2708	0.3292	0.2544
R_{16} (cm/%)	0.0	0.0	0.0	0.0
R_{23} (mr/cm)	3.5898	1.5690	−2.0086	−2.1067
R_{24} (mr/mr)	2.3859	1.2590	0.8011	−1.4028
R_{26} (mr/%)	−5.3493	−3.8518	−1.0358	3.4167
R_{31} (cm/cm)	1.2437	0.7851	0.7532	0.7475
R_{32} (cm/mr)	0.0	0.0	0.0	0.0
R_{36} (cm/%)	−10.0000	−10.0000	−10.0000	−10.0000
R_{41} (mr/cm)	0.6257	2.0442	6.0114	−0.2996
R_{42} (mr/mr)	0.8229	1.2695	1.2897	1.3123
R_{46} (mr/%)	5.9181	7.3479	−13.7723	56.6185

† Beam sizes calculated for phase spaces listed in Table 1.

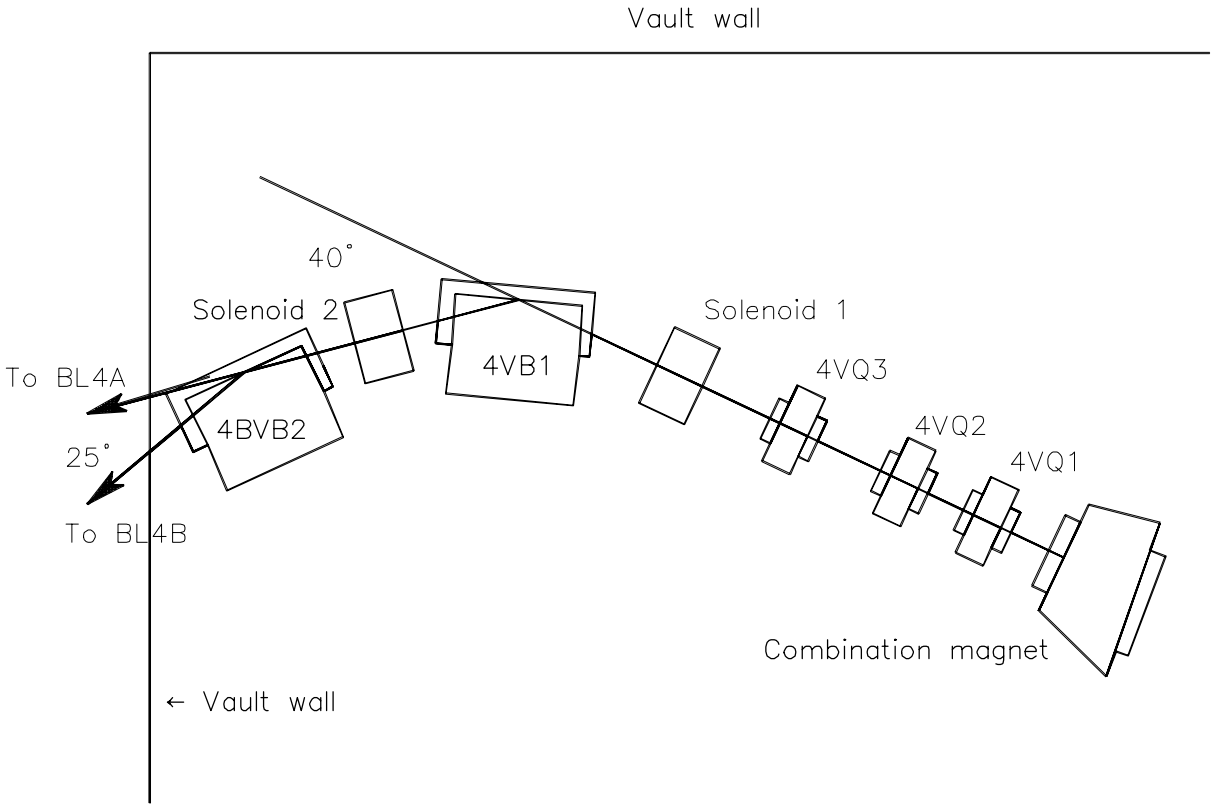

Fig. 1. Reconfiguration of the vault section of beam line 4 for longitudinal polarization.

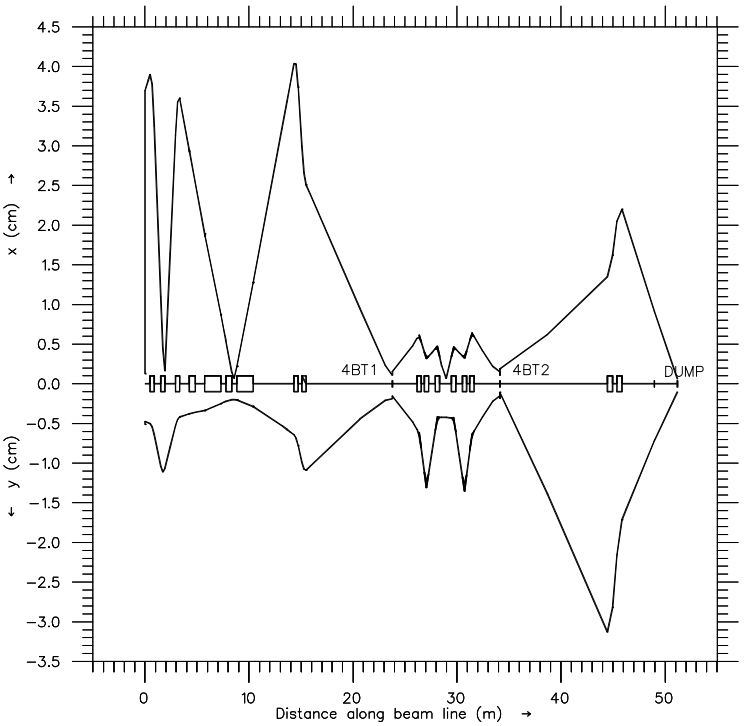

Fig. 2. 200 MeV beam profiles in the achromatic mode of operation.

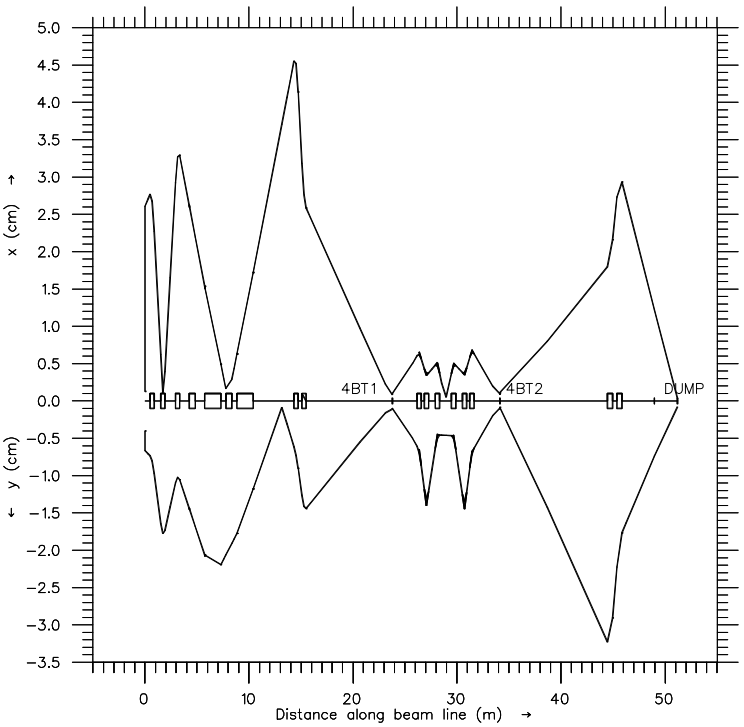

Fig. 3. 300 MeV beam profiles in the achromatic mode of operation.

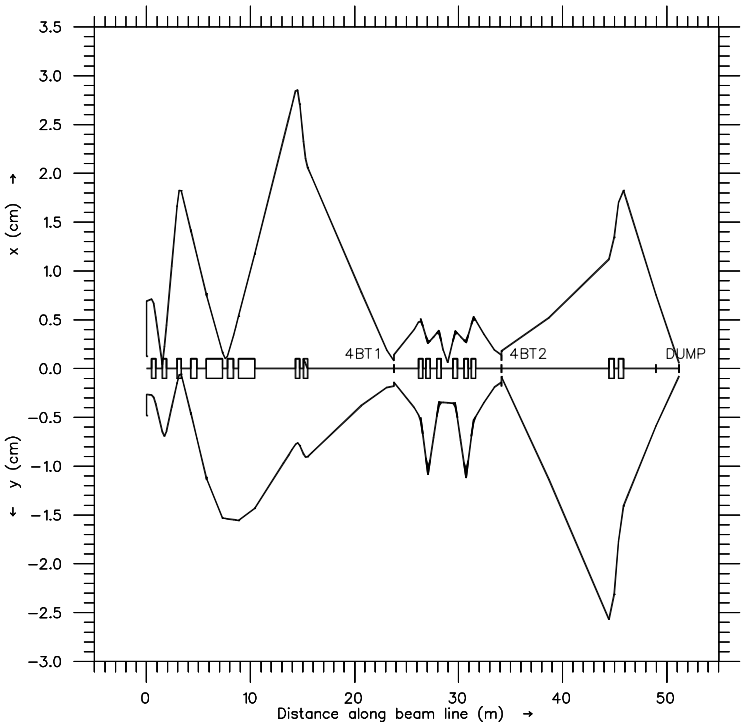

Fig. 4. 400 MeV beam profiles in the achromatic mode of operation.

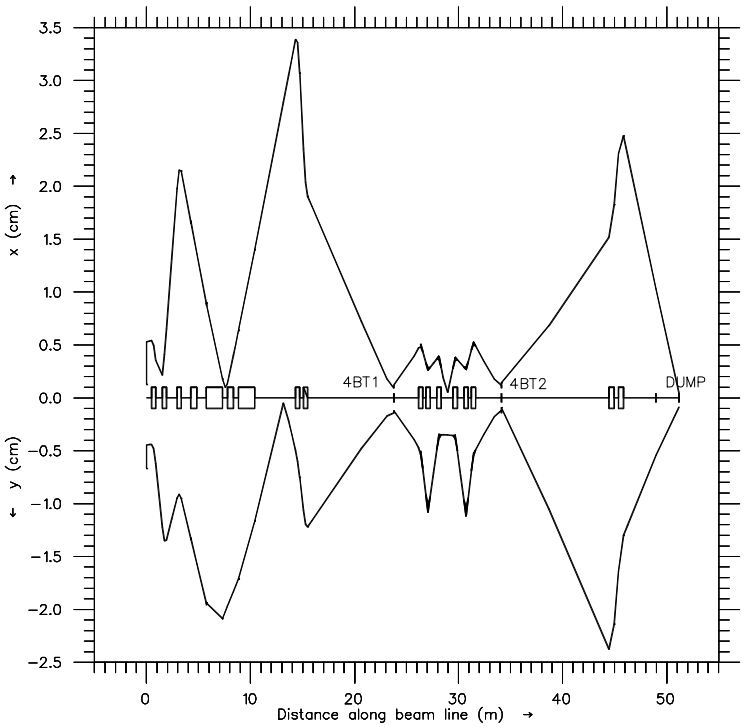

Fig. 5. 500 MeV beam profiles in the achromatic mode of operation.

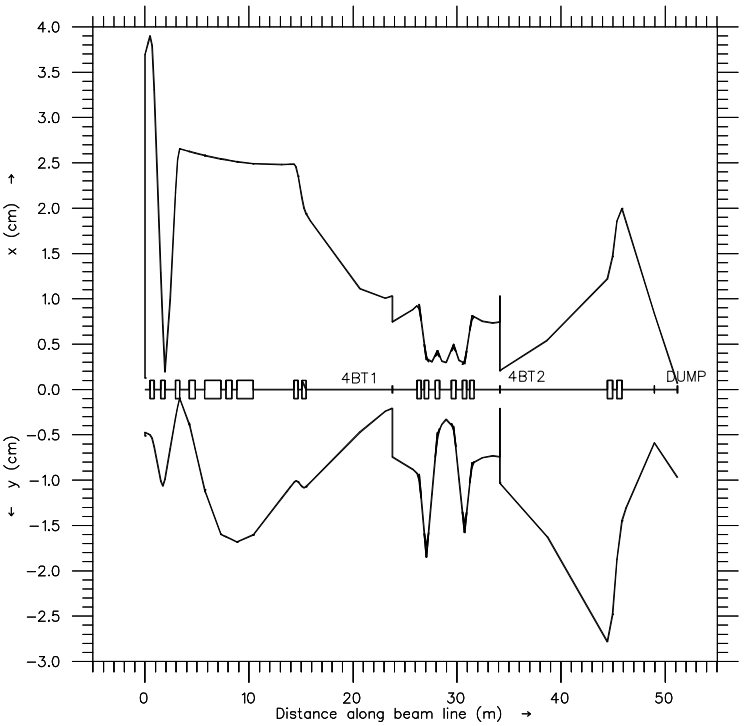

Fig. 6. 200 MeV beam profiles in the dispersed mode of operation.

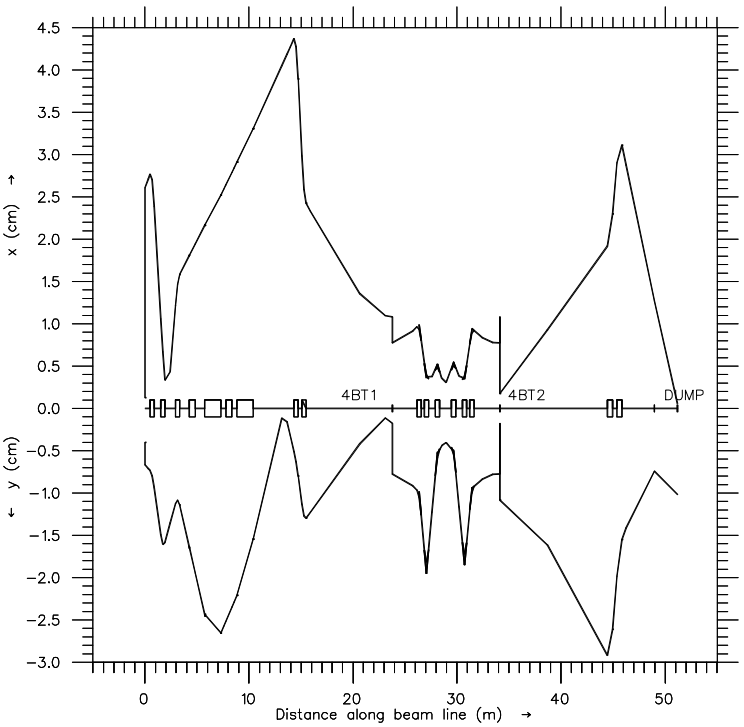

Fig. 7. 300 MeV beam profiles in the dispersed mode of operation.

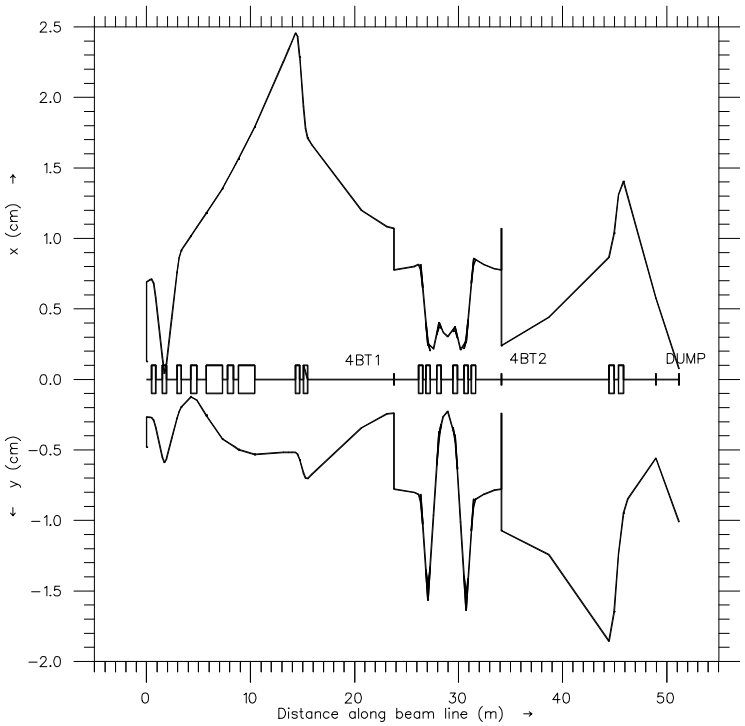

Fig. 8. 400 MeV beam profiles in the dispersed mode of operation.

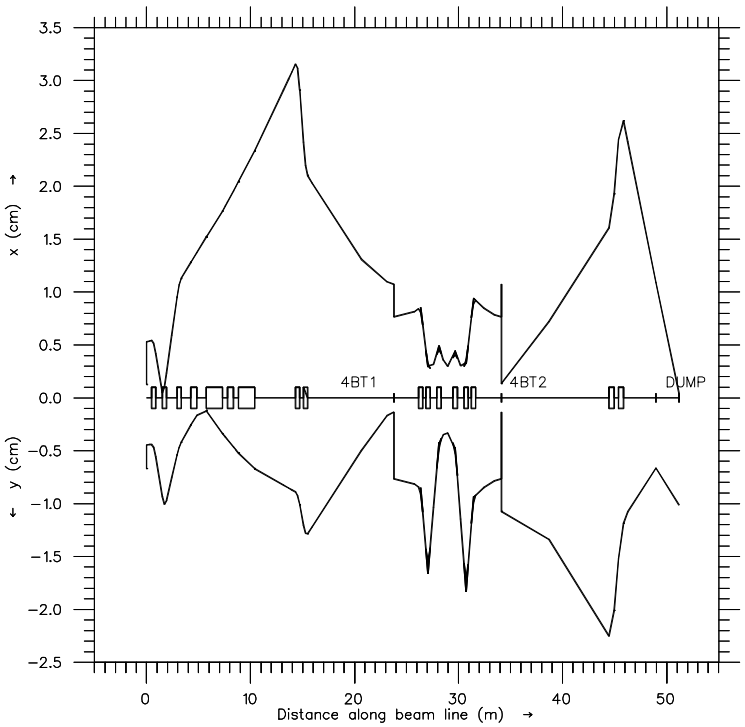

Fig. 9. 500 MeV beam profiles in the dispersed mode of operation.

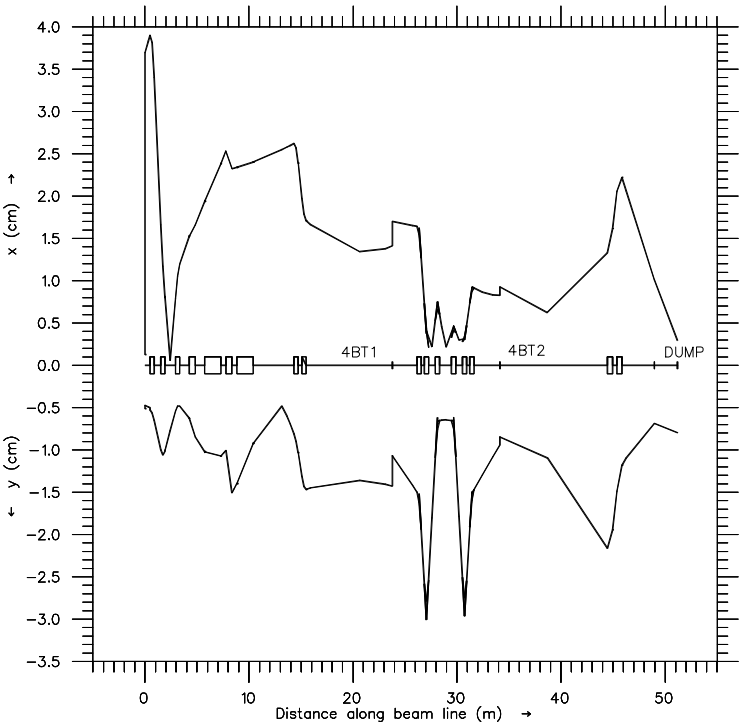

Fig. 10. 200 MeV beam profiles in the dispersed and solenoids on with vault quadrupole rotation.

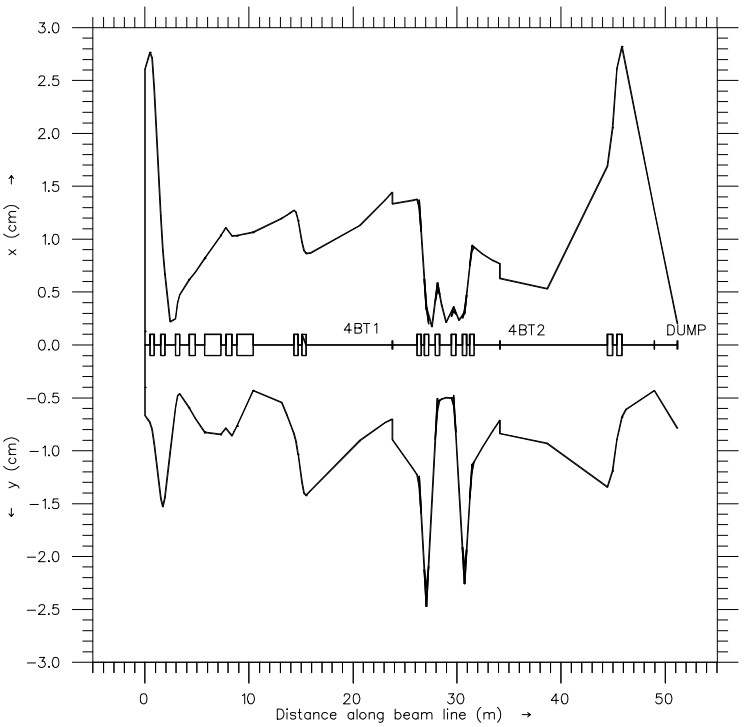

Fig. 11. 200 MeV beam profiles in the dispersed and solenoids on with vault quadrupole rotation.

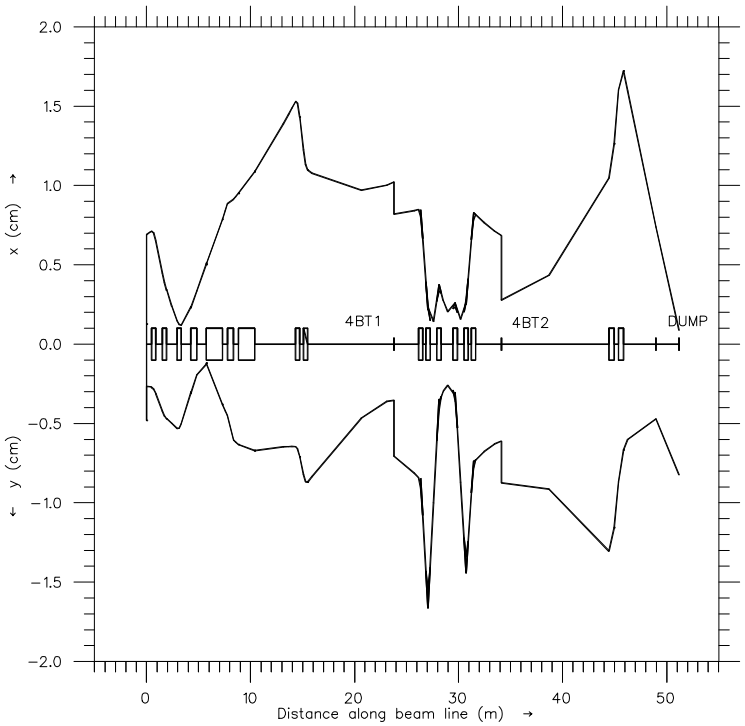

Fig. 12. 400 MeV beam profiles in the dispersed and solenoids on with vault quadrupole rotation.

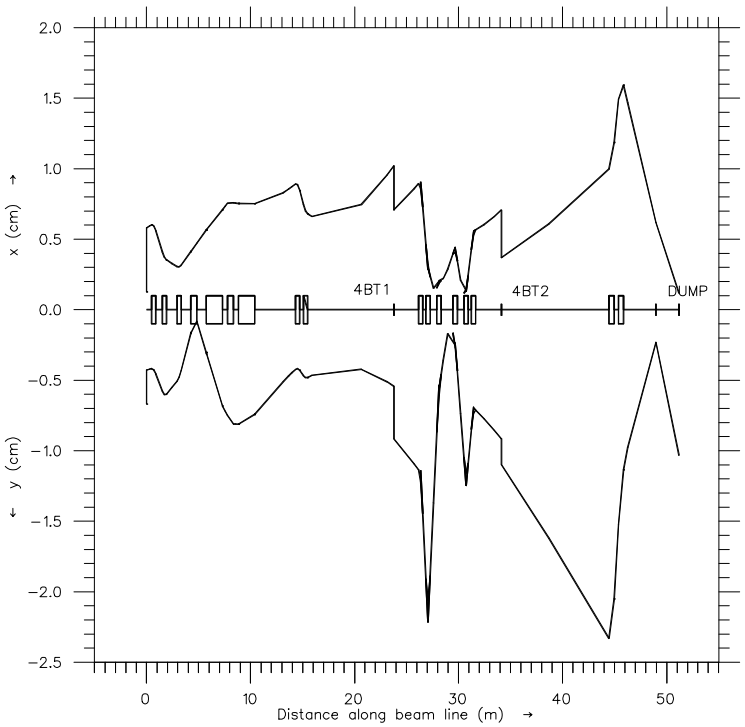

Fig. 13. 500 MeV beam profiles in the dispersed and solenoids on with vault quadrupole rotation.

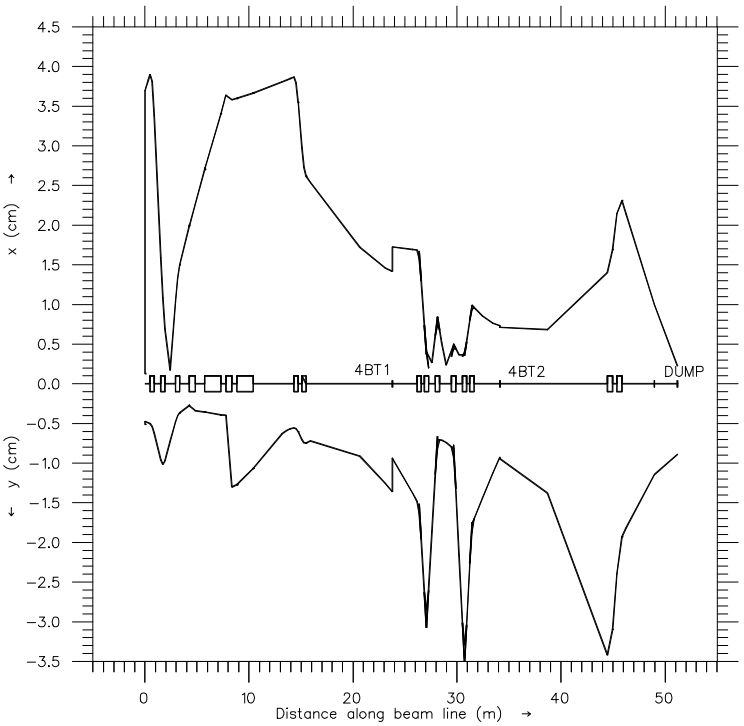

Fig. 14. 200 MeV beam profiles in the dispersed and solenoids on with no vault quadrupole rotation.

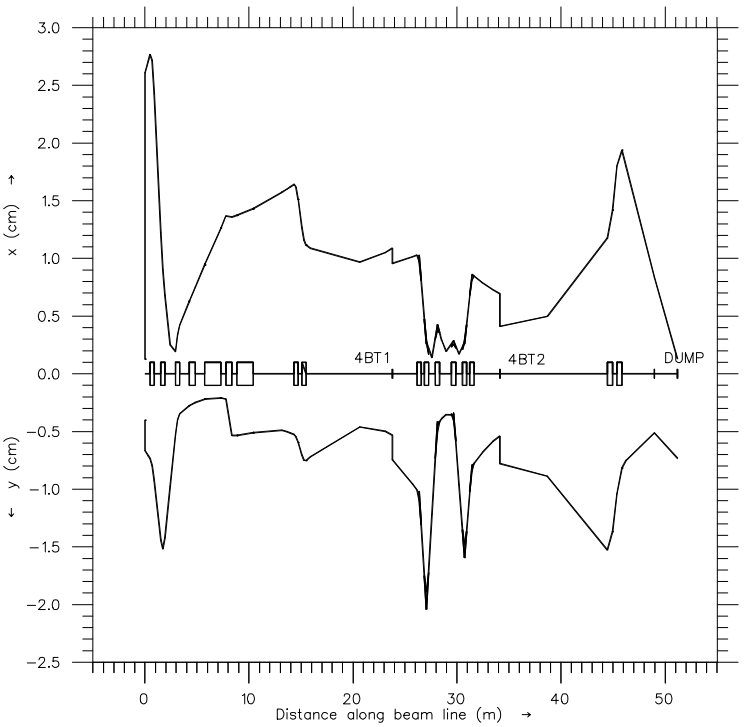

Fig. 15. 300 MeV beam profiles in the dispersed and solenoids on with no vault quadrupole rotation.

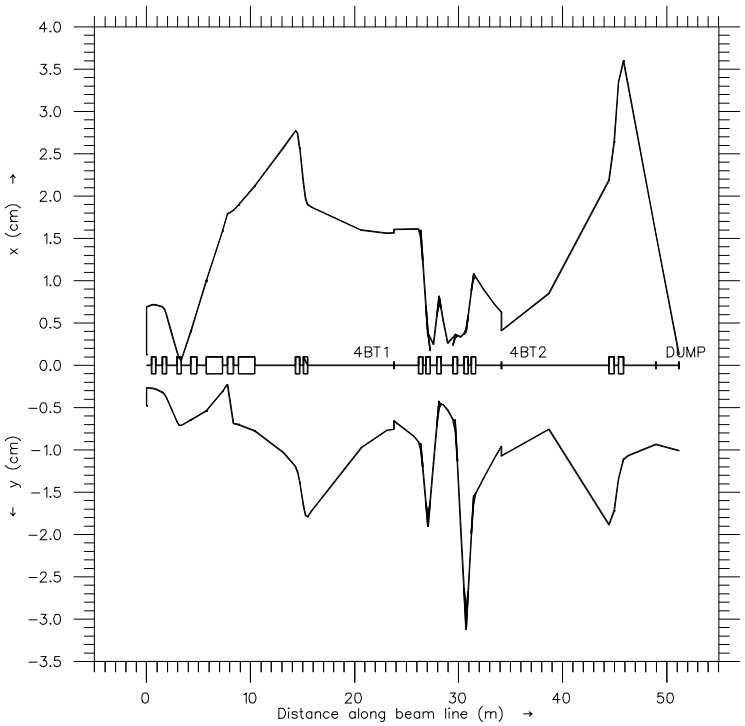

Fig. 16. 400 MeV beam profiles in the dispersed and solenoids on with no vault quadrupole rotation.

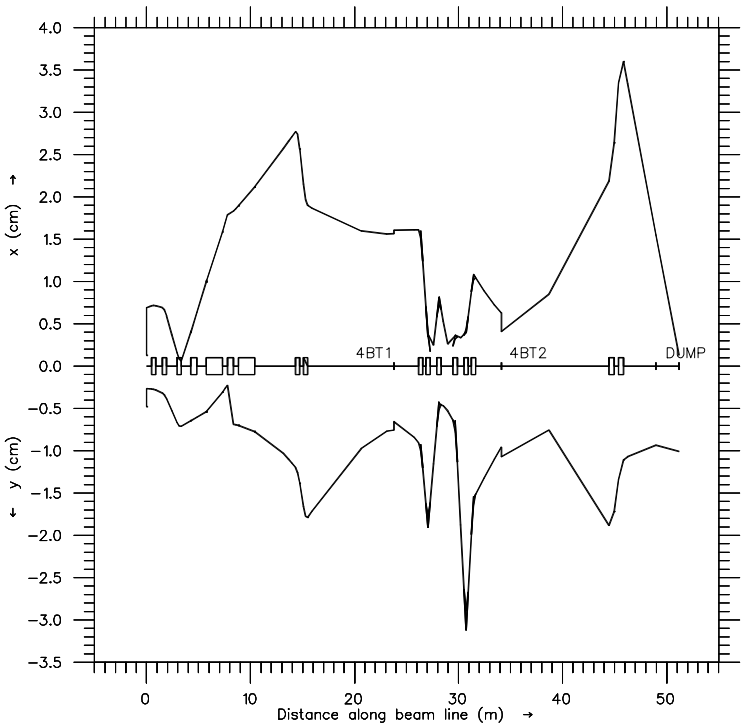

Fig. 17. 500 MeV beam profiles in the dispersed and solenoids on with no vault quadrupole rotation.

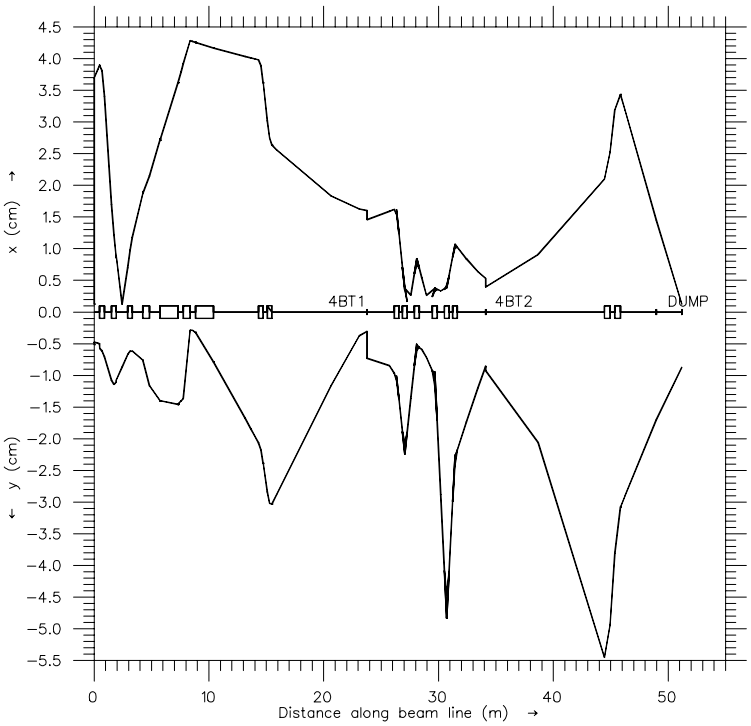

Fig. 18. 200 MeV beam profiles in the transverse mode of operation.

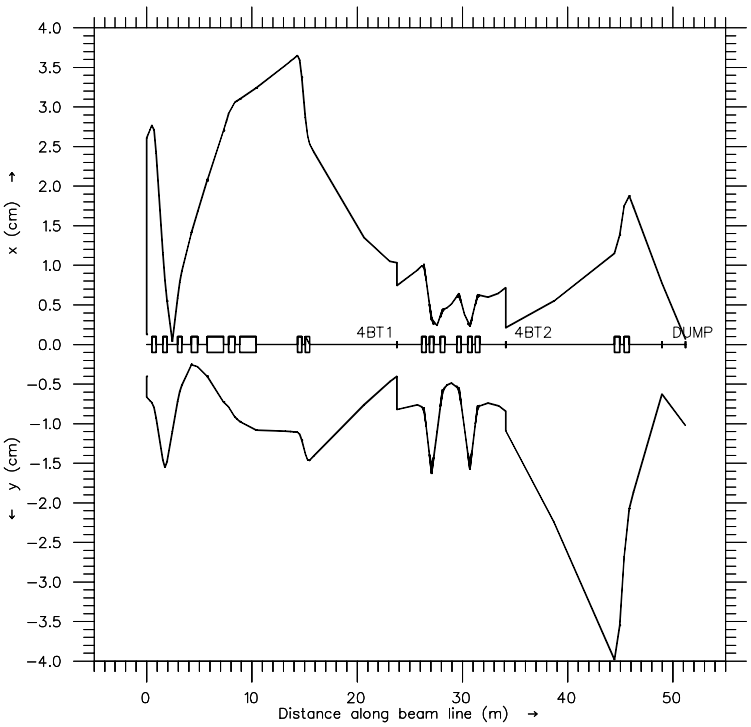

Fig. 19. 300 MeV beam profiles in the transverse mode of operation.

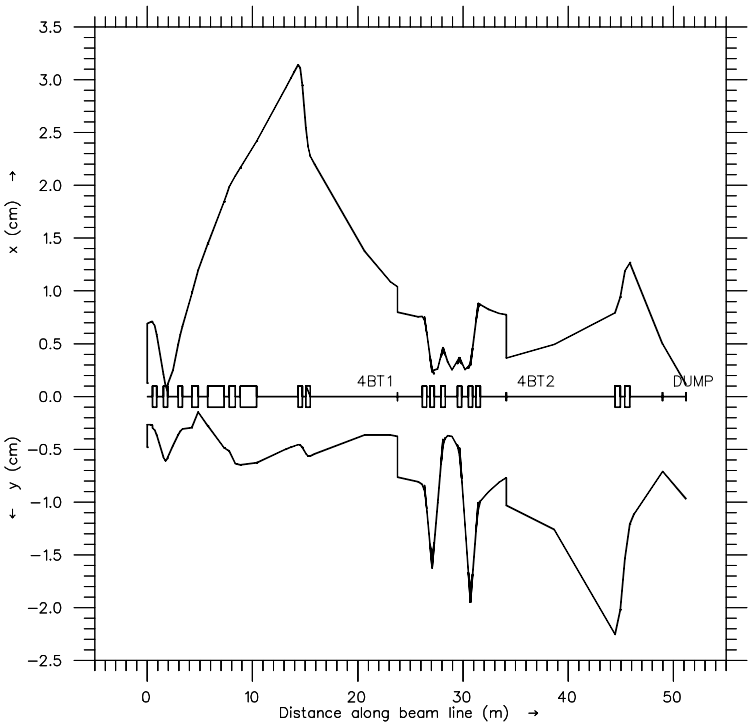

Fig. 20. 400 MeV beam profiles in the transverse mode of operation.

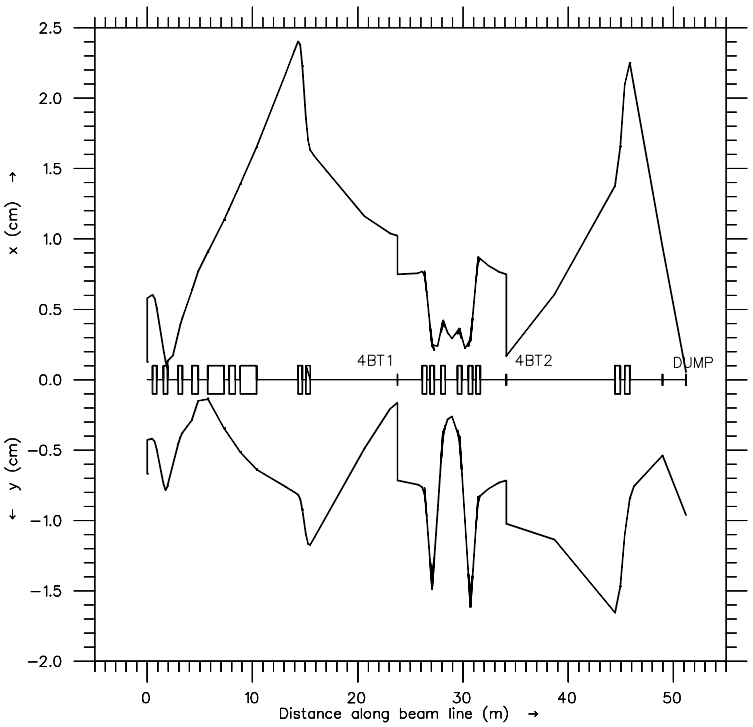

Fig. 21. 500 MeV beam profiles in the transverse mode of operation.